Korean J. Chem. Eng., **30**(11), 2100-2107 (2013)
DOI: 10.1007/s11814-013-0142-4

Photodegradation of 2,4,6-trinitrophenol catalyzed by Zn/MgO nanoparticles prepared in aqueous-organic medium

Shaista Ali, Muhammad Akhyar Farrukh†, and Muhammad Khaleeq-ur-Rahman

Department of Chemistry, GC University Lahore, Lahore 54000, Pakistan
(*Received 9 April 2013 • accepted 31 July 2013*)

Abstract−Synthesis of Magnesium oxide (MgO) nanoparticles and zinc deposited magnesium oxide (Zn/MgO) nanoparticles was carried out using hydrothermal and deposition-precipitation method with the variation of 1-Propanol (organic solvent) concentration, sodium hydroxide and urea concentration. The nanoparticles were characterized by using FTIR, TGA, SEM-EDX, TEM and XRD. The photocatalytic efficiency of MgO and Zn/MgO nanoparticles was studied by degradation of 2,4,6-trinitrophenol (TNP), which is highly acute and toxic and causes skin and eyes diseases, liver malfunction and tumor formation. Photodegradation of TNP was carried out under UV irradiation and confirmed by using HPLC and GC-MS. MgO and Zn/MgO nanoparticles that were synthesized by using urea showed higher first-order rate constant (k) value and percentage degradation as compared to nanoparticles that were synthesized using NaOH. It was observed that the concentration of solvent has direct relation with the k value of degradation of TNP.

Key words: Nanocatalysts, Zn/MgO, Trinitrophenol, Degradation, Pollutant

INTRODUCTION

MgO nanoparticles are highly efficient and active adsorbents for many toxic chemicals including air pollutants, chemical warfare agents, and acid gases (pH=1-7). Magnesium oxide has wide applications in the detection and remediation of chemical waste and warfare agents. It is used in superconducting and ferroelectric thin films as the substrate and has promising applications as both catalyst and catalyst support [1]. Destructive adsorption takes place on the surface of the nanoparticles, so that adsorbate remain chemically dismantled and thereby nontoxic. Recently, its degradation capability has been observed in different chemical warfare agents like diethylchlorophosphate (DECIP) [2], 2-chlorobenzene, 1,3 and 1,4-dichorobenzenes, 1,3,5-trichlorobenzene, dimethyl methylphosphate (DMMP), Sulfur mustard (bis-2-chloroehtyl sulphide) HD (2,2-dichloroethyl sulphide or known as mustard gas) [3], VX (*O*-ethyl, *S*-2-(diisopropylamino)ethylmethylphosphonothioate), GD (3,3-dimethyl-2-butyl methylphosphonofluoridate, or known as Soman) [4], diisopropylfluorophosphate (DFP), Hexafluoropropylene (HFP), Paraoxon [5] and Trimethyphosphite [6].

2,4,6-Trinitrophenol (TNP), a nitroaromatic compound (NAC), is highly reactive with a wide variety of the materials (e.g., concrete, plaster, amines, bases, and metals such as lead, zinc, copper, and mercury) to form phenolate salts, which are more reactive and also shock sensitive than the acid itself [7]. It is associated with many industrial chemical processes, environmental contaminants of industrial pollution and wastewater discharge. Some of the NACs possess mutagenic, carcinogenic and also toxic properties to the aquatic and terrestrial organisms. TNP is one of the main propellants that have been used as solid fuel oxidants for thruster and ammunitions. It has high toxicity risks and possible endocrine effects [8,9].

†To whom correspondence should be addressed.
E-mail: akhyar100@gmail.com

Several ways are being used for the destruction and degradation of NACs by sodium and silver zeolites, charcoal filter, and impregnated charcoals, but recently inorganic metal oxides show good capability and result in degradation of explosives. Conventionally, metal oxide powders of MgO, CaO, and Al_2O_3 possess little reactivity towards NACs, but their reactivity is anticipated to be enhanced with micro and especially in nanosized particles due to larger surface area of smaller particles [10]. Several methods like hydrothermal, conventional heating [11], anodization [12], deposition-precipitation method [13], wet oxidation method [14] and sol-gel method [15] are being applied to synthesize the nanoparticles. Recent studies showed that the efficiency of MgO nanoparticles as a catalyst is increased by deposition [16].

We prepared MgO nanoparticles by hydrothermal method, and deposited Zinc metal on MgO nanoparticles by the deposition-precipitation method. The effect of concentration of 1-propanol (dielectric constant), sodium hydroxyl and urea on the size of nanoparticles was studied. The catalytic efficiency of the MgO and Zn/MgO nanoparticles was investigated with and without photo irradiation of TNP at 25±1 °C.

EXPERIMENTAL WORK

1. Material and Apparatus

Magnesium chloride ($MgCl_2 \cdot 6H_2O$), 1-Propanol, Urea, Zinc Acetate dihydrate ($Zn(CH_3COO)_2 \cdot 2H_2O$) were purchased from Merck, Sodium hydroxide from Panreac and 2,4,6-trinitrophenol from Sigma-Aldrich. All chemicals were used without any further purification. For the synthesis auto Hydrothermal Teflon bomb, Ev 018 AC-Kapa-Vakummetre Oven and for calcination High Temperature Tube furnace (HTRH 70-600/18) was used.

The following instruments were used for characterization: FTIR (MIDAC M2000) was used to confirm the presence of MgO and Zn. TGA (SDT Q600 V8.3) analysis was done to find the water

Table 1. Variation in solvent concentration

Sr. no.	Solvent percentage/ %	1-Propnaol/ mL	Water/ mL	Solvent ratio
1	10	0.1	8.1	1 : 9
2	20	1.8	7.2	2 : 8
3	30	2.7	6.3	3 : 7
4	40	3.6	5.4	4 : 6
5	50	4.5	4.5	5 : 5

loss, and the maximum temperature for MgO and Zn/MgO nanoparticles was taken as 500 °C and 800 °C, respectively. XRD (X'pert PRO, PANalytical) was used to measure the particle size and crystallite phases. SEM (S-3400N- Hitachi) and FESEM (Unit Mikroskopi Elektron) analysis was used to find the morphology of nanoparticles. TEM (Phillip CM12 microscope) analysis was done to find the morphology and particle size of nanoparticles. Degradation of 2,4,6-trinitrophenol was confirmed by HPLC (LC 20 AT, Shimadzu) and GCMS (QP-2010, Shimadzu).

2. Synthesis of MgO Nanoparticles by Hydrothermal Method

MgO nanoparticles were prepared by taking different concentrations of solvent (1-propanol) and base. 182.97 mg (0.1 mol L^{-1}) of $MgCl_2 \cdot 6H_2O$ was used as a precursor and 180 mg (0.5 mol L^{-1}) of sodium hydroxide or 270 mg (0.5 mol L^{-1}) of urea was added to solvent having different concentration of water & 1-propanol (Table 1). The total amount of the solvent was taken as 9 mL.

The mixture was then stirred for 30 minutes. Then the mixture was transferred to the Teflon autoclave (hydrothermal bomb) and then kept in the oven for three hours at 150 °C. The resulting product was washed first with distilled water for several times via centrifugation (12,000 rpm) and then with methanol until the neutral pH was obtained. Neutral pH indicates the removal of impurities like unreacted base and hydrochloric acid (HCl). The product was allowed to dry overnight at room temperature. If some water content still remained, then the product was kept in the oven until it became dry. The product was subjected to calcination for 3 hours at 600 °C.

3. Synthesis of Zn/MgO Nanoparticles by Deposition-precipitation Method

MgO nanoparticles that were synthesized by using urea were used as a substrate to make a Zn deposited MgO nanoparticles. 29.969 mg of zinc acetate dihydrate (Zn $(CH_3COO)_2 \cdot 2H_2O$) was dissolved in 9 mL water, then 50 mg of MgO nanoparticles was added and the change in pH was noted before and after addition of MgO nanoparticles. The pH was adjusted by using 0.5 mol L^{-1} sodium hydroxide (NaOH) till the solution reached the pH 10 that is the IEP value for MgO [17]. The mixture was stirred for 30 minutes. After the stirring, the mixture was transferred to the hydrothermal bomb and then kept in the oven for three hours at 150 °C. The resulting product was washed and calcined as stated above. Five different samples of MgO nanoparticles were taken as a substrate, which were prepared in 10, 20, 30, 40, 50% 1-propanol concentration.

4. Catalytic Test

30 ppm solution of TNP was prepared by taking 10 mg of it in distilled water. Its spectrum was recorded with UV-Vis spectrophotometer to find λ_{max}. Two λ_{max} were observed at 356 and 208 nm; however, 356 nm wavelength was selected for study because of hav-

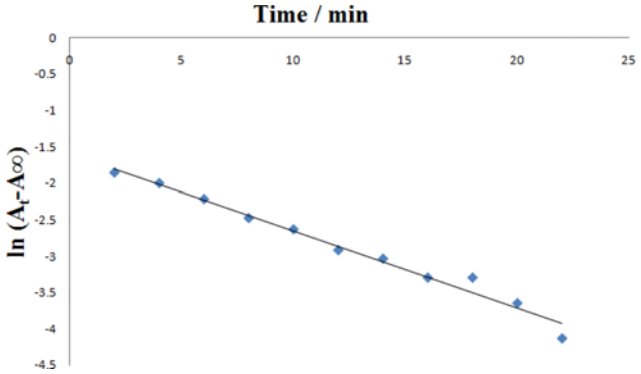

Fig. 1. First-order plot for the degradation of TNP.

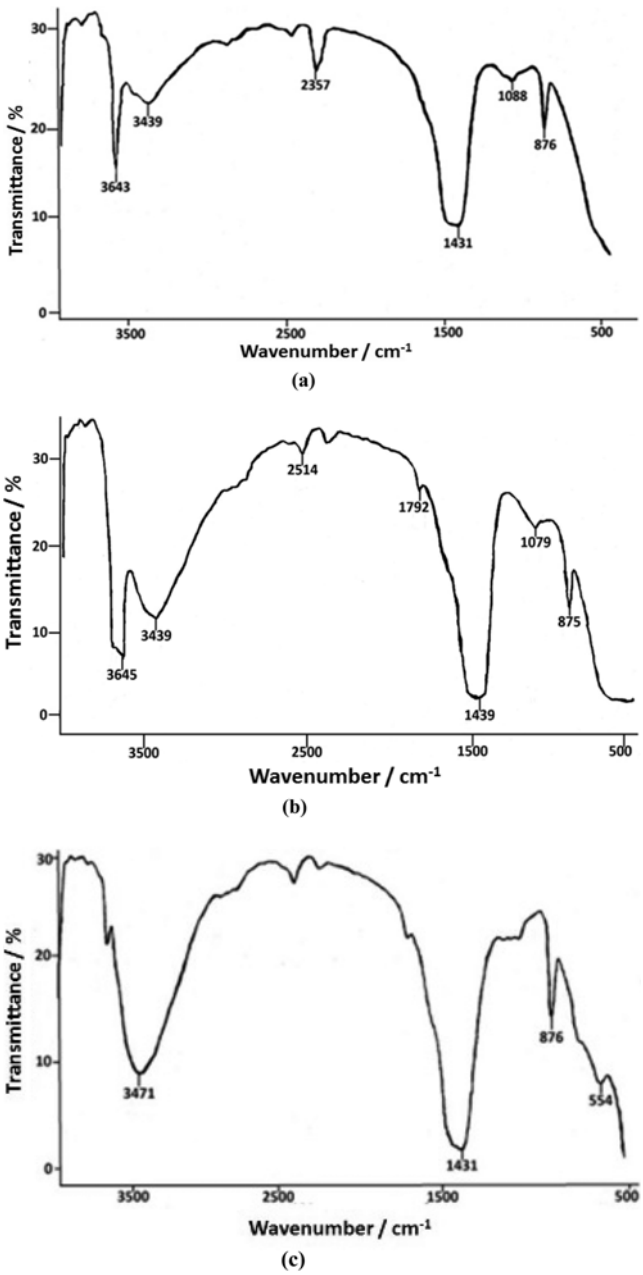

Fig. 2. FTIR spectra of MgO prepared using (a) NaOH (b) urea (c) FTIR spectra of Zn/MgO.

ing maximum absorbance. 5 mg of catalyst (MgO or Zn/MgO) was added in beaker having 25 mL of TNP solution. It was placed under UV light with constant stirring. The decrease in absorbance was observed by UV-visible spectrophotometer due to catalytic degradation of MgO and Zn/MgO. Graphs were plotted between $\ln(A-A_\infty)$ vs time using a first-order rate equation $\ln(A-A_\infty)=-kt+\ln[A]_o$. The value of rate constants k was calculated from the slope of the graphs (as shown in Fig. 1).

RESULTS AND DISCUSSION

1. Fourier Transform Infrared Spectroscopy

MgO nanoparticles and Zn deposited MgO nanoparticles were identified by FTIR. The peak obtained at 3,643 and 3,439 cm^{-1} was due to stretching vibration of -OH. The peaks obtained at 2,375, 1,431, 1,469 and 1,088 cm^{-1} show the presence of symmetrical unidentate carbonate (C-O) due to atmospheric adsorption of CO_2 on highly reactive surface area of these nanoparticles [18]. The main peak of Mg-O is present at 875 cm^{-1} [19]. Peak at 876 cm^{-1} was observed of MgO when synthesized using 30% solvent by using NaOH as a base (as shown in Fig. 2(a)) Peak at 875 cm^{-1} was observed due to MgO when synthesized using 30% solvent using urea (Fig. 2(b)). Fig. 2(c) shows the FTIR spectrum of Zn deposited on MgO nanoparticles; in addition to MgO peak, which is present at 876 cm^{-1}, an additional peak at 554 cm^{-1} was observed due to the presence of Zn deposition [20]. No absorption peak of Zn-O was observed at 430 cm^{-1} [21]. This indicates the presence of the Zn/MgO. The broad peaks round 3,471 cm^{-1} can be ascribed to stretching mode of bonded -OH with Zn [22].

2. Thermal Gravimetric Analysis (TGA)

Thermal gravimetric analysis was carried out at 500 °C. The result showed the loss of water and the decomposition behavior of the sample (Fig. 3(a)). The decomposition process of $Mg(OH)_2$ to MgO begins at about 345 °C and the strongest endothermic peak appears at 377 °C. The rate of mass loss from 98.5% at 345 °C to 72.5% at 430 °C, over 26% close to the conversion of $Mg(OH)_2$ to MgO, which indicates the end of the decomposition process [23]. In case of Zn deposited on MgO nanoparticles (Fig. 3(b)), the loss of water starts from 96.63% at 105.13 °C and ends at 68.70% at 671.97 °C. The loss of water molecules observed at 357 °C was 18.19%. This loss at higher temperature was due to the hydroxides molecules being strongly bonded with magnesium in magnesium hydroxides, and they require higher energy for decomposition as its calcination temperature varies from 400 to 1,200 °C [23].

3. Scanning Electron Microscope and Energy Dispersive X-ray (EDX) Analysis

SEM image displays the rod-like morphology of MgO when pre-

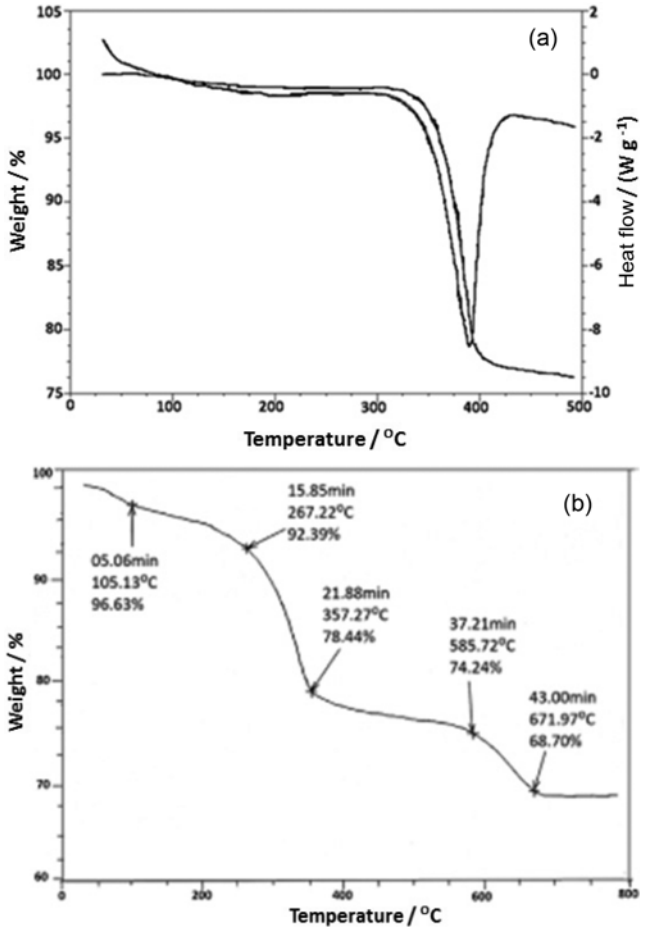

Fig. 3. TGA of (a) MgO (b) Zn/MgO.

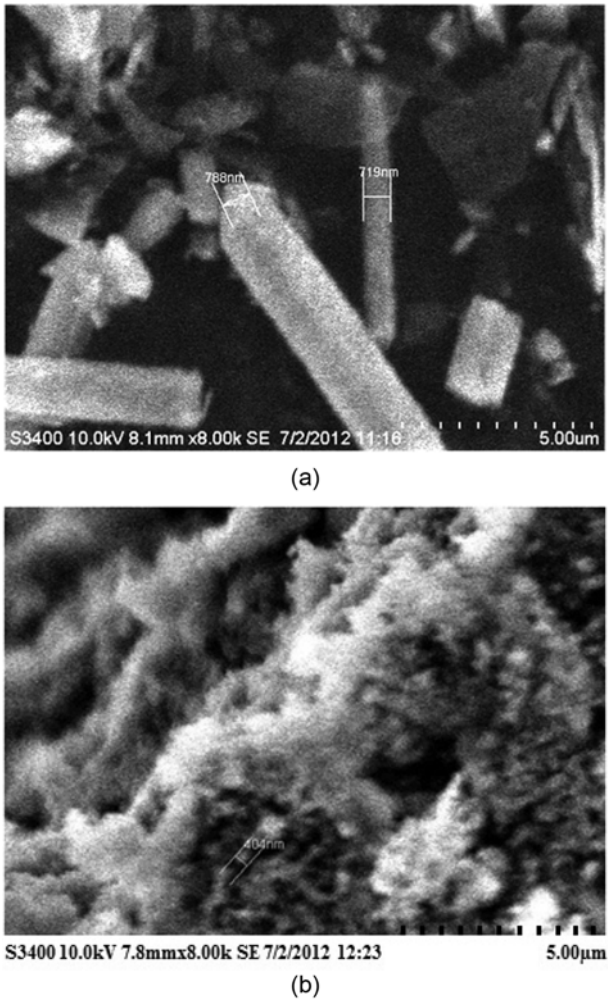

Fig. 4. SEM images showing (a) rod-like-structure of MgO using urea (b) agglomerated MgO using NaOH.

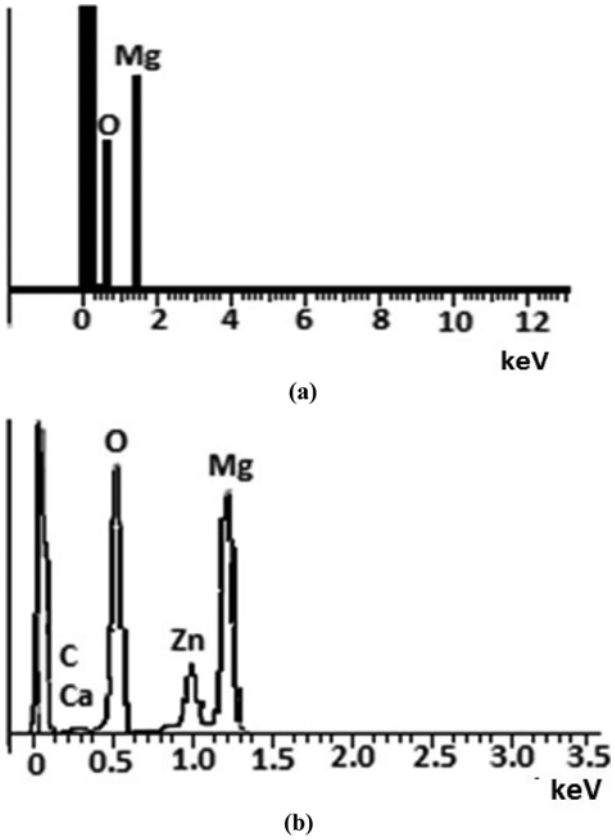

Fig. 5. EDX graph of (a) MgO (b) Zn/MgO.

pared by using urea as a base as shown in Fig. 4(a). However, MgO nanoparticles prepared using NaOH as a base show agglomerated morphology (Fig. 4(b)).

It shows that the base influenced the morphology of the particles because when NaOH was dissolved in water, a sudden increase in temperature was observed, which caused the formation of agglomerated nanoparticles. However, urea decomposes gently to produce OH^- ions, which results in the growth of rod-like nanoparticles [11]. Elemental composition of magnesium and oxygen was determined by using EDX analysis. The theoretical percentage of Mg in MgO nanoparticles is 60% and oxygen is 40%; the EDX results showed the percentage of Mg and O was from 55 to 63% and 36 to 45%, for all the five samples of MgO synthesized by changing solvent percentage as shown in Table 1. Fig. 5(a) shows EDX of MgO prepared by 30% solvent concentration.

FESEM images (Fig. 6(a) and (b)) show deposition of Zn on MgO nanoparticles. It was observed that loading of Zn in Zn/MgO nanoparticles prepared using 40% solvent concentration was more than Zn/MgO nanoparticles synthesized using 50% solvent concentration. Deposition of Zn was confirmed by EDX analysis (Fig. 5(b) Zn/MgO where MgO was synthesized by using 30% solvent concentration), which shows percentage loading of Zn on MgO nanoparticles that were prepared using different concentration of solvent and using urea. Percent loading of Zn was found to be 14.17, 13.39, and 5.25% in 30, 40 and 50% solvent concentration, respectively.

4. Transmission Electron Microscope (TEM) Analysis

TEM analysis (Fig. 7) was performed to determine the size and morphology of the nanoparticles, which looks like the surface of a

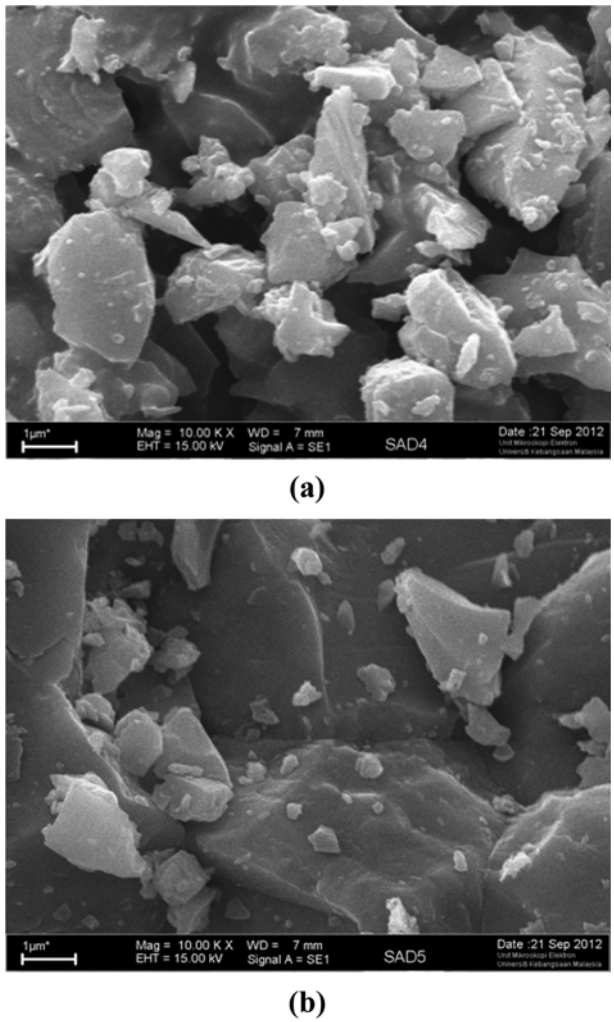

Fig. 6. FESEM images Zn/MgO prepared using solvent concentration (a) 40% (b) 50%.

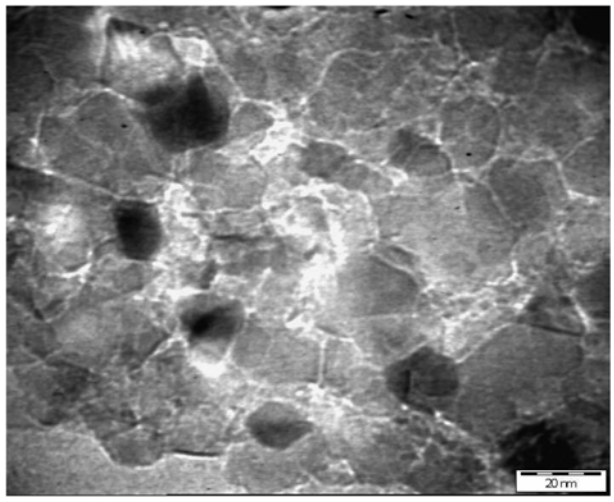

Fig. 7. TEM image of MgO nanoparticles.

big piece of crystal that includes many grains inside. The effect of solvent on particle size was measured and it was found that MgO nanoparticles showed decrease in particle size by increasing sol-

vent concentration. Particle size/grain size of MgO nanoparticles prepared in 30, 40, and 50% solvent concentration was found to be 21.98, 13.23 and 6.27 nm, respectively.

5. X-ray Diffraction (XRD) Characterization

The crystallite phases and size of nanoparticles were analyzed by X-ray diffraction (XRD). The particle size Zn/MgO nanoparticles was calculated by using the Scherrer equation. Fig. 8(a)) shows the XRD pattern of MgO [24]. 2-theta values at 29.19, 32.59, 37.12, 43.03, 48.29, 58.42 and 62.26 corresponding to the (111), (111), (210), (220), (220), (320) and (322) cubic planes of MgO. Zn was also confirmed by comparing XRD-spectra [25] (Fig. 8(b)), where 2-theta values at 29.70, 32.14, 36.31, 43.21, 47.11, 56.68, 62.10, and 70.08 correspond to the (100), (110), (110), (200), (200), (211), (220) and (221) having cubic structural phase. MgO nanoparticles showed 2-theta values of 32.59, 37.12, 43.03, 48.29 and 62.26 having 3.16, 6.37, 4.88, 6.03 and 5.33 nm, respectively, calculated by Scherer equation. Similar particle size was calculated at 2-theta values of Zn/MgO at 32.14, 36.60, 43.11, 47.73, and 62.10 having average particle size 0.89, 2.73, 1.78, 2.49 and 2.65 nm respectively. Particle size of MgO nanoparticles when prepared using urea as a base in 50% solvent concentration was calculated through TEM images and XRD at phase 220 and was found as 6.27 nm and 4.88 nm respectively, which is close to each other. However, for Zn/MgO nanoparticles, crystallite phase of 200 of XRD was used to calculate the particle size, which was found 1.78 nm. This shows that particle size decreases by deposition of Zn on MgO nanoparticles.

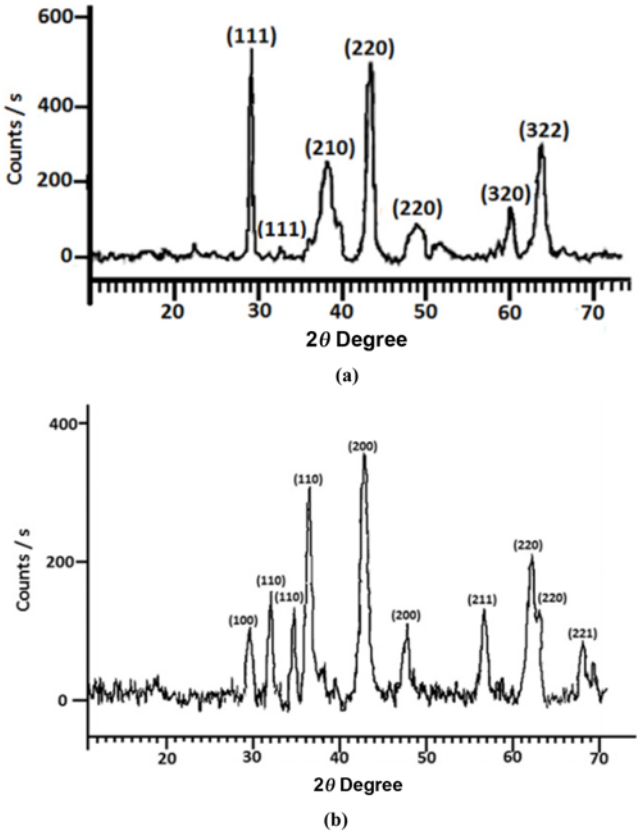

Fig. 8. XRD patterns of (a) MgO nanoparticles (b) Zn/MgO nanoparticles.

6. Photodegradation of TNP

6-1. Effect of Solvent

The effect of solvent on the synthesis of Zn and Zn/MgO nanoparticles was determined by using double sphere model of ion-ion interaction as given in Eq. (1). When two reactants (Z_AZ_B) possess same charges, then rate constant k will be directly proportional to dielectric constant (D) [26], but in our case both reactants (Zn^{+2} and OH^-) have opposite charges. The rate constant "k" would be inversely proportional to dielectric constant (D) due to opposite charges. The dielectric constant of water is 78.57 [27], while the 1-propanol has the value of 20.8 [28]. By increasing the concentration of 1-propanol, the dielectric constant decreases and the rate constant increases. This expresses that nucleation would complete at early stage, leading to small particle size, as confirmed by TEM and XRD. It was observed that by increasing the concentration of solvent, k value for the degradation of TNP increases.

$$\ln k = \ln k_o - e^2 Z_A Z_B / D r_{AB} K_B T \quad (1)$$

where D is the dielectric constant, k is specific rate constant for ion-ion interactions, k_o is specific rate constant at zero ionic strength and infinite D, K_B is Boltzmann's constant, r is radius of activated complex, T is temperature, e is charge on electron and Z_A Z_B are valence of ions A and B.

In all the three sets (Table 2) solvent had a major effect on the

Table 2. Degradation of TNP by using MgO & Zn/MgO nanoparticles

Solvent percentage/ %	Set 1*		Set 2†		Set 3A‡		Set 3B§	
	Time of degradation/ minutes	k/ min^{-1}	Time of degradation/ minutes	k/ min^{-1}	Time of degradation/ minutes	k/ min^{-1}	Time of degradation/ minutes	k/ min^{-1}
10	120	0.022	148	0.055	48	0.141	18	0.068
20	114	0.107	54	0.085	46	0.105	30	0.094
30	100	0.038	62	0.153	40	0.105	22	0.107
40	94	0.049	50	0.322	28	0.14	42	0.039
50	124	0.023	27	0.003	---------	--------	15	0.305

* Set 1=MgO nanoparticles prepared by using NaOH as a base

† Set 2=MgO nanoparticles prepared by using Urea as a base

‡ Set 3A=Degradation of TNP using Zn/MgO nanoparticles in the presence of UV-light

§ Set 3B=Degradation of TNP using Zn/MgO nanoparticles without using UV-light

degradation efficiency of nanocatalysts. As the particle size of nanoparticles decreases, k value increases due to the large surface area where adsorption could occur. By comparing Set 1 and Set 2 we can see that Set 2 shows the increase in k value from 0.055 to 0.322 min^{-1} as compared to Set 1, i.e., from 0.022 to 0.049 min^{-1} by changing the concentration of solvent from 10 to 40%. The last sample that is of highest solvent concentration 50% shows least "k value" in both cases: 0.023 min^{-1} in Set 1 and 0.003 min^{-1} in Set 2.

The MgO of Set 2 with 50% solvent concentration prepared by using urea shows the particle size up to 6.5 nm as per observed by TEM. It has a very small size; perhaps because of its very small size it will degrade quickly before even data can be observed accurately, as its degradation time is also less as compared to Set 1. Time of degradation also greatly affects by increasing the concentration of the solvent as shown in Table 2.

By comparing both Sets (Table 2) it could be concluded that Set 2 shows less time of degradation compared to Set 1 which is from 148 to 27 minutes.

6-2. Effect of Deposition

In case of Set 3 where Zn metal was deposited on MgO nanoparticles, the degradation was studied by using two ways: by placing the sample in UV irradiation (Set 3A) and without UV irradiation (Set 3B). The k values were found to increase as compared to Set 2, that is, from 0.055 to 0.141 min^{-1} (for 10% solvent concentration) and decrease in time of degradation from 148 to 48 minutes (for 10% solvent concentration) and increase in percentage degradation.

It was observed that in degradation of TNP with Zn/MgO using as a catalyst under UV irradiation, the k value increases from 0.141 to 0.14 min^{-1} as compared to without UV irradiation from 0.067 to 0.039 min^{-1} but in last sample using 50% Zn/MgO, which shows highest k value, (0.305 min^{-1}), maximum percentage degradation (45%) and less time of degradation (15 minutes) required without UV irradiation. This sample was considered to be the best sample as it shows maximum percentage degradation and highest k value.

6-3. Effect of Base

Effect of base (Set 1 and Set 2) was studied by preparing MgO nanoparticles in the presence of sodium hydroxide and urea. An increase in k value from 0.055 to 0.322 min^{-1} was observed by using urea (Set 2) as compared to the k value from 0.022 to 0.049 min^{-1} when prepared in NaOH (Set 1) as shown in Table 2.

6-4. Degradation Mechanism

Degradation of TNP was confirmed by using HPLC and GCMS.

For High Performance Liquid Chromatography (HPLC): Three solutions of TNP were prepared a) without using any nanocatalysts, b) with 05 mg of MgO nanocatalysts, c) with 05 mg of Zn/MgO nanocatalyst. C18 column was used for separation of the components and the mobile phase used was as 70% methanol whose pH was maintained at 3.4. Volume of 20 μL of the sample was injected [29] Peak heights and retention time of sample a and b, a and c were compared for identification of degradation of TNP. The peaks at a specific retention time are observed for blank in Fig. 9(a) and for samples in Fig. 9(b) and (c). The peak of TNP was observed (Fig. 9(a)) sharp at retention time of 7.425 min. But no peak was observed at 7.425 of TNP in reaction of sample b and c, which indicates that TNP is degraded but is present in very minute concentrations so its peak is not visible. Peaks observed at 3.93, 3.92 and 9.42 min retention time (as shown in Fig. 9(b) and (c)). This indicates that degraded products are present.

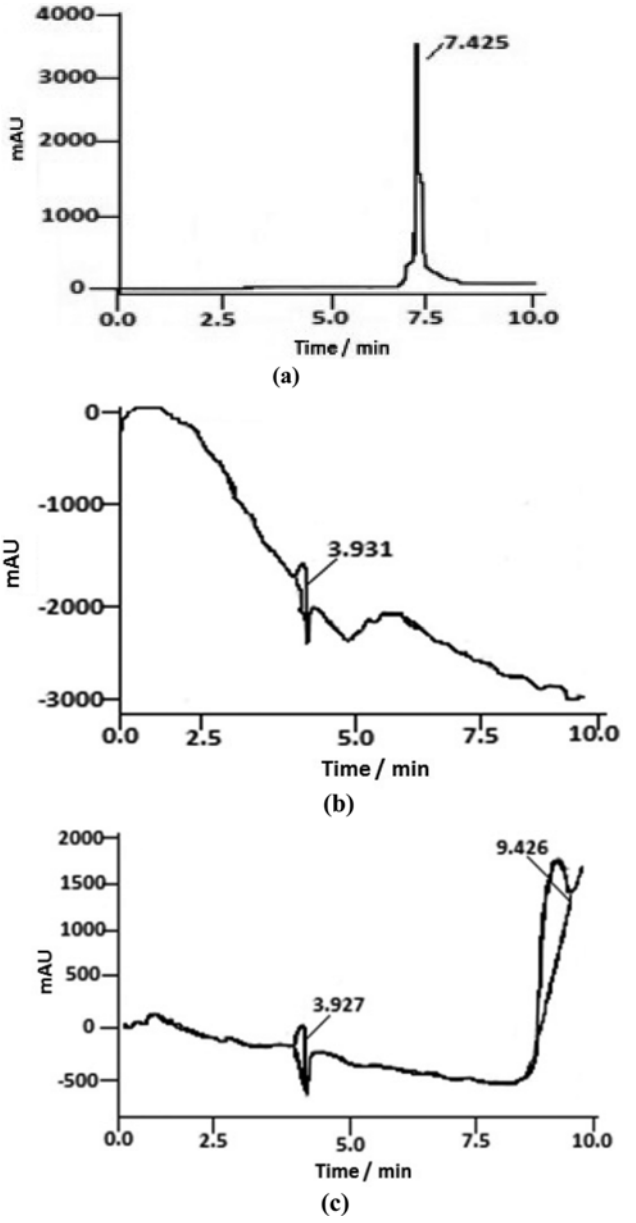

Fig. 9. Chromatogram of (a) blank (TNP) at a specific retention time (without nanocatalyst) (b) degraded product of TNP at a specific retention time (with Zn/MgO catalyst) (c) degraded product of TNP at a specific retention time (with MgO catalyst).

Gas chromatography mass spectrometry (*GC-MS*) was also used to observe the degradation of TNP. By the catalytic action of MgO nanoparticles, TNP is degraded as no peak was observed at 229 m/e of TNP (molecular mass of TNP) as shown in Fig. 10 because of low concentration and less intensity of remaining un-degraded TNP. A number of peaks having a molecular weight in the range from 200 to 430 were found [30].

Based on the above evidence, a graphical representation may be shown in Fig. 11 which highlights the mechanism starting from the synthesis of nanocatalysts to the degradation of TNP.

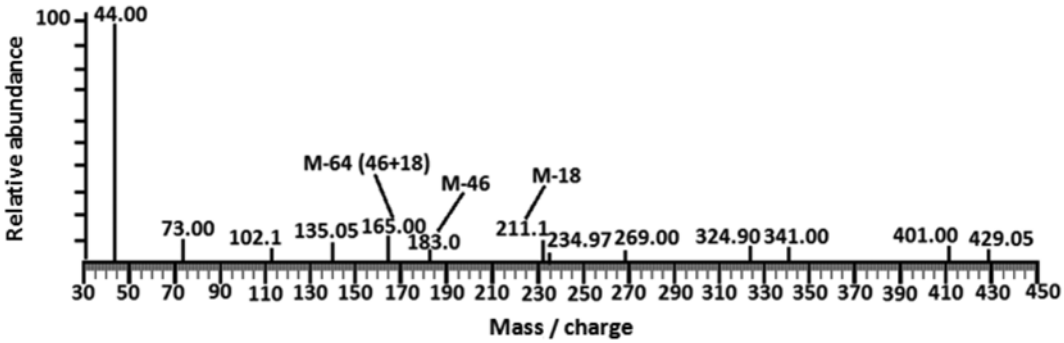

Fig. 10. GCMS spectrum of degraded TNP using MgO as a catalyst.

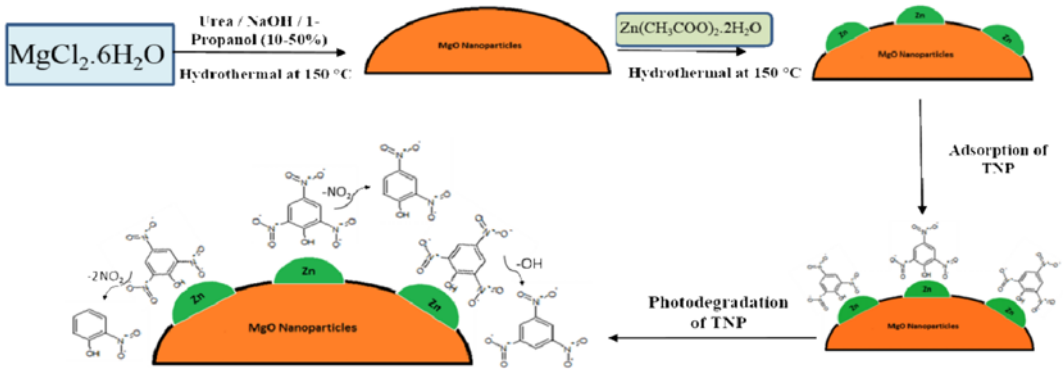

Fig. 11. Mechanism of degradation of TNP.

CONCLUSION

Solvent-controlled synthesis of MgO nanoparticles and Zn/MgO nanoparticles shows that by increasing the concentration of solvent, the size of nanoparticles decreases (size was decreased up to 6.27 nm observed via TEM) and k value increases. Time of degradation is also affected by increasing concentration of solvent, as by increasing solvent concentration the time of degradation decreases, as in all three sets time span is less for that sample having a maximum concentration of solvent, e.g., 15 minutes for Set 3B. Rod-like structures of MgO nanoparticles were formed when urea was used as a base, and increase in k value and decrease in time of degradation were observed. Zn/MgO shows 45% percentage degradation of TNP as compared to MgO nanoparticles having 12.18%. It was also observed that Zn/MgO acts as a better catalyst without UV irradiation of TNP.

ACKNOWLEDGEMENT

The World Academy of Sciences (TWAS) is gratefully acknowledged for the financial support through research grant (11-028 RG/MSN/AS_C; UNESCO FR: 3240262649). Department of Physics, GC University Lahore is acknowledged for providing TGA and XRD facilities.

REFERENCES

1. H. Mirzael and A. Davoodnia, *Chin. J. Catal.*, **33**, 1502 (2012).
2. A. Saxena, H. Mangal, P. K. Rai, A. S. Rawat, V. Kumar and M. Datta, *J. Hazard. Mater.*, **180**, 566 (2010).
3. M. E. Martin, R. M. Narske and K. J. Klabunde, *Micropor. Mesopor. Mater.*, **83**, 47 (2005).
4. R. M. Narske, K. J. Klabunde and S. Fultz, *Langmuir*, **18**, 4819 (2002).
5. S. Rajagopalan, O. Koper, S. Decker and K. J. Klabunde, *Chemistry*, **8**, 2602 (2002).
6. Y. X. Li, O. Koper, M. Atteya and K. J. Klabunde, *J. Mater. Chem.*, **4**, 323 (1992).
7. W. O. Cooper, *Explosives Engineering*, Wiley-VCH, New York (1996).
8. H. Stucki, *Chimia*, **58**, 409 (2004).
9. J. A. Bullock, *Introduction to Homeland Security*, Elsevier Butterworth-Heinemann, USA, 147 (2006).
10. C. G. Granqvist, R. A. Buhrman, J. Wyns and A. J. Sievers, *Phys. Rev. Lett.*, **37**, 625 (1976).
11. M. A. Farrukh, B. T. Heng and R. Adnan, *Turk. J. Chem.*, **34**, 537 (2010).
12. H. S. Goh, R. Adnan and M. A. Farrukh, *Turk. J. Chem.*, **35**, 375 (2011).
13. H. Yazid, R. Adnan, S. A. Hamid and M. A. Farrukh, *Turk. J. Chem.*, **34**, 639 (2010).
14. K. M. A. Saron, M. R. Hashima and M. A. Farrukh, *Appl. Surf. Sci.*, **258**, 5200 (2012).
15. R. Adnan, N. A. Razana, I. A. Rahman and M. A. Farrukh, *J. Chin. Chem. Soc.*, **57**, 222 (2010).
16. M. Kong, Q. Yang, W. Lu, F. Zheyong, J. Fei, X. Zheng and T. D. Wheelock, *Chin. J. Catal.*, **33**, 1508 (2012).
17. M. Kosmulski, *Chemical properties of material surface*, Marcel

Dekker, Inc., New York, 65 (2001).
18. O. B. Koper, I. Lagadic, A. Volodin and K. J. Klabunde, *Chem. Mater.*, **9**, 2468 (1997).
19. L. Z. Pei, W. Y. Yin, J. C. Wang, C. G. Fan and Q. F. Zhang, *Mater. Res.*, **13**, 339 (2010).
20. J. Bang, H. Yang and P. H. Holloway, *Nanotechnology*, **17**, 973 (2006).
21. X. B. Qiang, D. Hua, D. Y. Nian and Y. T. Bin, *T. Nonferr. Metal. Soc.*, **17**, 671 (2007).
22. T. Subbaiah, S. C. Mallick, I. N. Bhattacharya, S. Anand and R. P. Das, *The European Journal of Mineral Processing and Environmental Protection*, **4**, 1303 (2004).
23. A. Becheri, M. Durr, P. L. Nostro and P. Baglioni, *J. Nanopart. Res.*, **10**, 679 (2008).
24. J. D. Hanawalt, H. W. Rinn and L. K. Frevel, *Anal. Chem.*, **10**, 475 (1938).
25. C. Suryanarayana and M. G. Norton, *X-ray diffraction: A practical approach*, Springer, USA, 129 (1998).
26. I. Muneer, M. A. Farrukh, Shagharf, M. Khaleeq-ur-Rahman, A. A. Umar and R. Adnan, *Mater. Sci. Forum*, **756**, 197 (2013).
27. F. H. Darke, G. W. Pierce and M. T. Dow, *Phy. Rev.*, **35**, 613 (1930).
28. J. H. Lee, J. Je, J. Hur, M. A. Schlautman and E. R. Carraway, *Analyst*, **128**, 1257 (2003).
29. K. Ashley and P. F. O. Connor *NIOSH manual of analytical methods*, Ed. 4, Method No. S228, NIOSH Publication, USA (1994).
30. M. Nipper, Y. Qian, R. S. Carr and K. Miller, *Chemosphere*, **56**, 519 (2004).